Available online at www.sciencedirect.com
ScienceDirect
Journal of Power Sources 161 (2006) 256–263
JOURNAL OF POWER SOURCES
www.elsevier.com/locate/jpowsour

Analysis of performance losses of direct ethanol fuel cells with the aid of a reference electrode

Guangchun Li *, Peter G. Pickup

Department of Chemistry, Memorial University of Newfoundland, Elizabeth Avenue, St. John's, Newfoundland, Canada A 1B 3X7

Received 24 February 2006; received in revised form 17 March 2006; accepted 28 March 2006
Available online 5 May 2006

Abstract

The performances of direct ethanol fuel cells with different anode catalysts, different ethanol concentrations, and at different operating temperatures have been studied. The performance losses of the cell have been separated into individual electrode performance losses with the aid of a reference electrode, ethanol crossover has been quantified, and CO_2 and acetic acid production have been measured by titration. It has been shown that the cell performance strongly depends on the anode catalyst, ethanol concentration, and operating temperature. It was found that the cathode and anode exhibit different dependences on ethanol concentration and operating temperature. The performance of the cathode is very sensitive to the rate of ethanol crossover. Product analysis provides insights into the mechanisms of electro-oxidation of ethanol.

Keywords: Fuel cell; Ethanol; Performance analysis; Reference electrode

1. Introduction

The development of direct ethanol fuel cells (DEFCs) has drawn increasing attention in recent years due to the attractive advantages of ethanol as a fuel [1–11]. Most importantly, ethanol is a renewable fuel, since it can be easily produced from agricultural products and biomass. It can be classified as a green fuel, because the carbon dioxide produced by ethanol fuel cells is consumed by biomass growth. Relative to hydrogen, ethanol is easily transported and stored, and its theoretical energy density of ca. 8.0 kWh kg^{-1} is comparable to that of gasoline.

Previous research has shown that the performance of DEFCs is quite promising. For example, Wang et al. [11] reported that at a high temperature of 170 °C, the performance of a DEFC was close to that of a direct methanol fuel cell when Pt/Ru was used as the anode catalyst. Arico et al. [2] found that with Pt/Ru as the anode catalyst, a maximum power density of 110 mW cm^{-2} could be obtained for a DEFC at 145 °C. More recent research [4,5,7,9,10] has been focused on lower temperature operation, which is more sustainable. Pt/Sn has consistently emerged as the best anode catalyst, giving maximum power densities of 30 mW cm^{-2} at 60 °C [9] and ca. 50–60 mW cm^{-2} at 90 °C [4,5,7,9], with pure O_2 as the oxidant. A wide variety of other catalysts have been investigated for ethanol oxidation [3,4,12–16], including ternary alloys [7,17–22], but none have yet surpassed the performance of Pt/Sn in DEFCs.

Despite the progress that has been made, the performance of DEFCs is much inferior to that of hydrogen fuel cells due to the slow kinetics of ethanol oxidation on state of the art catalysts. Although the thermodynamic equilibrium potential for ethanol oxidation is only 0.084 V versus SHE [1], electro-oxidation of ethanol is much slower than that of hydrogen and involves multiple pathways. Large amounts of side products, particularly acetaldehyde and acetic acid, have been found during electro-oxidation of ethanol. A recent differential electrochemical mass spectrometry study using a commercial carbon supported Pt catalyst has shown that the activity for complete oxidation remains low (2–13% current efficiency) over a range of ethanol concentrations (0.001–0.5 M) and temperatures (23–60 °C) [16]. Acetic acid and acetaldehyde were the major products, with current efficiencies ranging from 32% to 72% and from 15% to 66%, respectively. Alloying Pt with Ru [13,23], Sn [24,25], Mo [13], Os [26], or Re [4] lowers the overpotential for ethanol oxidation, and influences product distribution. Ru, Sn, Rh [14], Os, and Mo have been shown to increase the selectivity for CO_2 formation.

* Corresponding author. Tel.: +1 709 737 2648; fax: +1 709 737 3702.
E-mail address: guangchunli@yahoo.com (G. Li).

0378-7753/$ – see front matter © 2006 Elsevier B.V. All rights reserved.
doi:10.1016/j.jpowsour.2006.03.071

There are a limited number of reports on product analysis from DEFCs and the available data show wide variations. Arico et al. [2] have reported a 96% conversion of ethanol to CO_2 for a DEFC operating at 145 °C, and Zhou et al. [5] report that at 90 °C "CO_2 and acetic acid were the main products with PtSn/C and PtRu/C". On the other hand, Wang et al. [11] have reported that acetaldehyde was the major product at 170 °C, and Song et al. [10] reported that the amount of CO_2 produced at the anode of a DEFC was "quite small" at 90 °C. Their product analysis by GC showed 95% acetic acid: 5% acetaldehyde at a PtSn/C anode and 73% acetic acid: 27% acetaldehyde at a PtRu/C anode. Production of trace amounts of ethyl acetate has also been reported [5,10,11]. In light of these very limited and conflicting results, there is a need for further work on product analysis from DEFCs. Achieving high conversions to CO_2 is the greatest challenge facing the development of DEFCs.

Crossover of ethanol is also a serious issue affecting the performance and viability of DEFCs. This problem has been studied in depth for methanol fuel cells [27], and many potential solutions have been investigated [1,28]. Song et al. [8,29] have estimated ethanol crossover rates from the current required to oxidize ethanol crossing over to the cathode of a DEFC. They found that the increased crossover resulting from use of ethanol concentrations above 1 M, caused a sharp drop in the maximum power that could be obtained from the DEFC. Paganin et al. [30] have reported that 2 M ethanol produces a larger drop in open circuit potential, due to crossover, than 2 M methanol.

It is clear from the above review of the literature that development of high performance DEFCs depends on optimization of all of their components as well as their operating conditions. Although this complex task can be simplified by the availability of detailed information on individual potential losses at the anode and cathode, such an approach has not been reported, although it is gaining broader use in the development of methanol cells [31]. We therefore report here on the separation of cell performance losses in a DEFC into the cathode and anode losses with the aid of a dynamic hydrogen (DHE) reference electrode. Ethanol crossover has been measured, different anode catalysts, ethanol concentrations, and operating temperatures have been explored, and products (CO_2 and acetic acid) have been analyzed by titration, in order to build a complete picture of the factors influencing the performance of the cell.

2. Experimental

2.1. Materials

Nafion 115 and 117 membranes (DuPont) were cleaned at 80 °C with 3% H_2O_2, 1 M H_2SO_4(aq) and deionized water, and stored in deionized water. 20% Pt on XC-72 carbon (E-Tek Inc.), 20% Pt/Ru (1:1) on XC-72 carbon (E-Tek Inc.), carbon fibre paper (CFP) (Toray, 0.26 mm), and all other materials were used as received. Electrodes included 4 mg cm^{-2} Pt black on carbon paper (donated by Ballard Power Systems), 4.5 mg cm^{-2} Pt/Ru (1:1) black on carbon paper (donated by H. Power Corp.), and home-made carbon supported Pt/Sn (4:1) and Pt/Ru/Pb (1:1:0.3) catalysts on carbon paper.

The Pt/Sn (4:1) and Pt/Ru/Pb (1:1:0.3) catalysts were prepared by decoration of commercial 20% Pt on XC-72 carbon and 20% Pt/Ru (1:1) on XC-72 carbon (E-Tek Inc.) catalysts with Sn or Pb. In brief, 30 mg of the commercial catalyst was dispersed in deionized water by stirring, then an appropriate amount of $SnCl_2$ or $Pb(NO_3)_2$ dissolved in deionized water was added dropwise, followed by reduction with $NaBH_4$.

2.2. Preparation of anodes

An appropriate amount of catalyst was mixed with 200 mg of 5% Nafion solution by sonication for 30 min. The resulting paste was then applied onto a 5 cm^2 square of CFP and dried at ambient temperature in a fume hood, giving a metal loading of 2 mg cm^{-2}.

2.3. Preparation of membrane and electrode assemblies (MEAs)

Membrane and electrode assemblies were prepared by pressing an anode and a cathode (Pt black, 4 mg cm^{-2} on carbon paper, donated by Ballard Power Systems) onto each side of a Nafion 117 membrane at a pressure of 200 kg cm^{-2} at 135 °C for 180 s.

2.4. Fuel cell measurements

A 5 cm^2 commercial cell (ElectroChem) was used to perform fuel cell tests. The cell was operated with an anode feed of aqueous ethanol solution at a fixed flow rate of 5 ml min^{-1} and a cathode feed of dry air at a fixed flow rate of 60 ml min^{-1}. For product analysis, the cell was operated with an anode feed of 1 M ethanol(aq) at a fixed flow rate of 0.30 ml min^{-1} and a cathode feed of dry air at a fixed flow rate of 30 ml min^{-1}.

Electrochemical measurements were made with a Solartron 1286 electrochemical interface coupled with a 1250 frequency response analyzer or an EG&G PAR 273 A potentiostat/galvanostat.

2.5. Configuration of the reference electrode

We have designed a DHE reference electrode to measure single electrode potentials of hydrogen and methanol fuel cells [31]. The configuration of the DHE reference electrode is shown in Fig. 1. In this configuration, the working electrode and counter electrode of the DHE were placed on the cathode side of an outer section of the Nafion membrane and sandwiched between the two halves of the body of the cell. The distance between the thin Pt wire (100 μm diameter) electrodes of the DHE and the edge of the active electrodes of the fuel cell was much larger than three times the thickness of the membrane to avoid potential gradients. A small current of typically ca. 6×10^{-5} A was passed between the two Pt wires to maintain the hydrogen coverage on the cathode, which was used as the DHE reference electrode. Except for the two ends, the fine Pt wires were insulated with a thin coating of poly(vinyl chloride). The current to the DHE was supplied by a 9 V battery and controlled by adjusting the

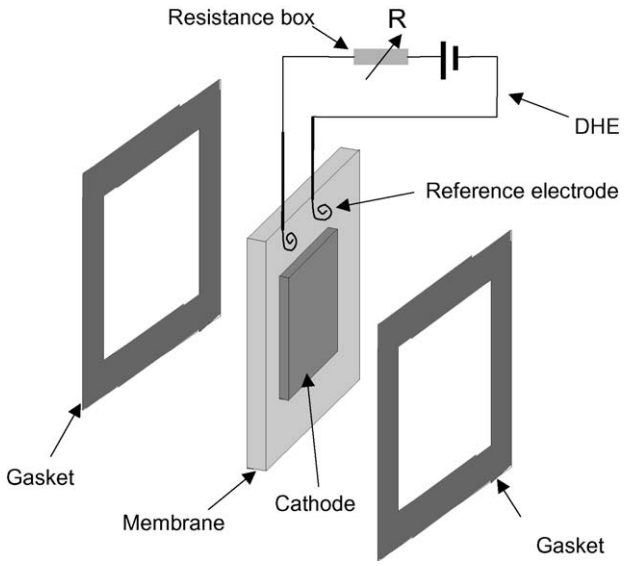

Fig. 1. Schematic diagram of a cell with a DHE reference electrode.

series resistance with a resistance box. Before measurements, the cell was fed with humidified hydrogen on the anode and the potential of the DHE reference electrode was set to zero with respect to the hydrogen anode by changing the series resistance.

It was found that in this configuration the DHE reference electrode was quite stable during polarization measurements of ethanol fuel cells at low current densities. At high current densities, a small drift (<15 mV) of the potential of the DHE reference electrode was observed. However, this drift is minor compared to anode and cathode overpotentials which were always larger than 300 mV at high current densities. In addition, the DHE reference electrode was regularly calibrated relative to hydrogen passing through the anode compartment to correct for any drift.

The good stability of the DHE reference electrode was also demonstrated by the closeness of the cell polarization curve to the cathode potentials (versus DHE) – anode potentials (versus DHE) (Fig. 5). Note that the anode potentials (versus DHE) and the cathode potentials (versus DHE) were measured at different times.

2.6. Measurements of ethanol crossover

Ethanol crossover was measured by following the electrochemical procedure developed by Ren et al. for measurement of methanol crossover [32], and recently used by Song et al. for measuring ethanol crossover [29]. In brief, one side of the cell was fed with aqueous ethanol while the other side was fed with humidified N_2. Ethanol permeating through the membrane to the N_2 side was oxidized electrochemically. The limiting ethanol oxidation current, measured after a period of 10 min at a potential of +0.9 V versus the cathode, was used as a measure of ethanol crossover. The current was not significantly dependent on potential between 0.8 V and 1.0 V, indicating that a true limiting current was obtained at 0.9 V. In these experiments, the cathode (ethanol solution side) evolves H_2 and approximates a dynamic hydrogen reference electrode.

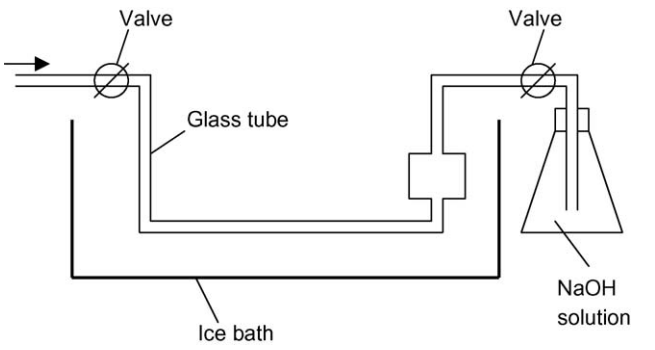

Fig. 2. Schematic diagram of the equipment for collecting the anode outlet solution and CO_2.

2.7. Analysis of DEFC products

The DEFC anode outlet solution was collected in a glass tube bathed in ice to reduce the volatility of the solution and the CO_2 was absorbed in an aqueous NaOH trap (Fig. 2). The CO_2 was determined by a two-step titration of the aqueous NaOH solution with standardized HCl [33,34]. The first step, with phenolphthalein as the indicator, converts sodium carbonate to sodium bicarbonate and consumes the excess NaOH. The second step, with methyl orange as the indicator, converts sodium bicarbonate to carbonic acid. The moles of sodium bicarbonate equals the moles of the CO_2 produced by ethanol oxidation on the anode of the DEFC. Non-volatile acids (mainly acetic acid) in the anode outlet solution were determined by titrating the solution with standardized NaOH. It was found that purging the solution collected in the glass tube with N_2 did not significantly influence either the amount of CO_2 collected, or the acid content of the solution.

3. Results and discussion

3.1. Ethanol crossover

The limiting ethanol oxidation current was used as a measure of ethanol crossover. It was found that the limiting ethanol oxidation current strongly depended on the membrane thickness, ethanol concentration, and cell operating temperature as reported in Tables 1 and 2. These results are consistent with the limiting current measured being a true representation of the amount of ethanol crossing the membrane. If the current were limited by the kinetics of ethanol oxidation, it would not depend the thickness of the membrane. However, it is not possible to entirely rule out some influence from the electron transfer kinetics.

Table 1
Ethanol crossover currents at 80 °C

Ethanol concentration(aq) (M)	Crossover current (A cm^{-2})	
	Nafion 115	Nafion 117
0.5	0.050	0.027
1	0.086	0.048
2	0.13	0.065

Table 2
Ethanol crossover currents (1 M ethanol) at different temperatures

Temperature (°C)	Crossover current (A cm^{-2})
23	0.0060
50	0.015
80	0.048

It was found that ethanol crossover was decreased greatly with the thicker membrane. For example, with a Nafion 117 membrane (ca. 175 μm), ethanol crossover was reduced to ca. half of that with a Nafion 115 membrane (125 μm). The larger than expected decrease in crossover can be attributed to slightly different characteristics of the membrane samples [35]. Also, ethanol crossover increased significantly with increasing ethanol concentration as expected. With a Nafion 117 membrane, increasing the ethanol concentration from 0.5 M to 1 M resulted in ca. a two times increase in ethanol crossover. Another finding is that ethanol crossover increased dramatically with increasing temperature. When the temperature was increased from room temperature to 80 °C, the crossover current increased from 0.006 A cm^{-2} to 0.048 A cm^{-2}, an eight-fold increase.

These results are similar to those reported by Song et al. [29], who observed crossover currents of 39–62 mA cm^{-2} at 75 °C for 1 M ethanol and Nafion 115. This compares with a value of 86 mA cm^{-2} at 80 °C in Table 1. It is also instructive to compare the results with those for methanol crossover under similar conditions. For Nafion 115, the crossover current for 1 M methanol in our cell at 60 °C was 92 mA cm^{-2} [35], similar to the value for 1 M ethanol at 80 °C. This indicates that ethanol oxidation in the crossover experiments was quite inefficient, resulting in less than six electrons per molecule (assuming similar permeabilities for methanol and ethanol). This is consistent with the product distributions reported below for ethanol oxidation at the anode, since acetaldehye and acetic acid formation are two and four electron processes, respectively.

3.2. Product analysis

The products of ethanol oxidation were analyzed by titration and the results are listed in Table 3. The cell was operated at 80 °C with an anode feed of 1 M ethanol(aq) and a cathode feed of dry air. It has been assumed here that the acid collected in the cold trap was exclusively acetic acid, since there has been no suggestion in the literature that significant quantities of other organic acids are produced.

Under all conditions studied, the major product of ethanol oxidation was acetic acid. Large amounts of acetaldehyde must also have been produced at 60 mA cm^{-2} with both catalysts [10,13,25], and these are estimated by difference in Table 3. It is also likely that trace amounts of ethyl acetate would have been produced in these experiments [5,10,11].

It is seen from the data in Table 3 that at a current density of 60 mA cm^{-2}, the yields of CO_2 were ca. 9.4% for the Pt/Sn catalyst and ca. 6.2% for the Pt/Ru catalyst. At a lower current density of 20 mA cm^{-2}, the yield of CO_2 was ca. 9.0% for the Pt/Sn catalyst. The clear conclusion from these data is that under these operation conditions, CO_2 is not the main product of ethanol oxidation, and the yield of CO_2 did not change significantly with cell voltage.

In addition, we can see that for the Pt/Sn catalyst, at the higher current density, the yield of acetic acid was ca. 48%, while at the lower current density, the yield of acetic acid was ca. 94%. For the Pt/Ru catalyst, the yield of acetic acid increased from ca. 60% to ca. 77% when the current density was decreased from 60 mA cm^{-2} to 30 mA cm^{-2}. This indicates that the yield of acetic acid varied greatly with cell voltage and catalyst.

These results are consistent with previously reported results on low temperature (<100 °C) DEFCs. Acetic acid production was similar to that reported by Song et al. [10] at 95 °C, and their difference between PtRu and PtSn (see Section 1) parallels ours at low current density (Song's measurements were made at 0.5 V). We have presumably obtained more than the "quite small" amount of CO_2 that they report. Our result with PtSn at low current is consistent with Zhou et al.'s [5] vague report of CO_2 and acetic acid as the main products. It is curious that the PtSn catalyst gave a lower yield of acetic acid than the PtRu catalyst at high current density, although the difference is perhaps not significant. It is pertinent that the cell potential was very low and similar in both cases (Table 3), due to the low ethanol flow rate used in the experiments to facilitate product analysis. It is likely that both anodes behave like Pt electrodes at the resulting high anode overpotentials.

The data reported in Table 3 are currently the most comprehensive available for low temperature DEFCs, and will form a valuable reference point for further work aimed at improving the yield of CO_2. It is noted that at 20 mA cm^{-2}, the sum of CO_2 and acetic acid corresponded to a little over 100% of the

Table 3
Product analysis for ethanol oxidation on a 20% Pt on C based Pt/Sn (4:1) catalyst and a Pt/Ru (1:1, 4.5 mg cm^{-2}) black catalyst at constant current for 1 h

	Pt/Sn				Pt/Ru			
Current (mA cm^{-2})	60	60	20	20	20	60	60	30
Cell voltage[a]	121	139	356	378	402	137	176	281
CO_2 (%)	8.4	10.4	8.4	10.1	8.4	6.7	5.6	6.7
Acetic acid (%)[b]	45.2	50.7	98.0	93.6	94.4	55.6	64.8	76.8
Acetaldehyde (%)[c]	46.4	38.9	0	0	0	37.7	29.6	16.5

[a] There was a small variation in the cell voltage during constant current operation, generally within ca. ±10 mV.
[b] Assuming that acetic acid was the only organic acid produced.
[c] Calculated by difference, by assuming that CO_2, acetic acid, and acetaldehye were the only significant products.

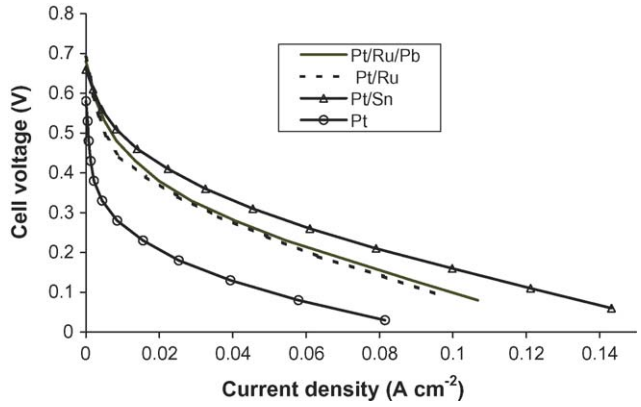

Fig. 3. Polarization curves for a DEFC with different anode catalysts. The catalysts include 20% Pt on C from E-Tek, 20% Pt/Ru (1:1) on C from E-Tek, 20% Pt on C based Pt/Sn (4:1), and 20% Pt/Ru (1:1) on C based Pt/Ru/Pb (1:1:0.3). The cell was operated at 80 °C with an anode feed of 1 M ethanol(aq) and a cathode feed of dry air.

charge passed. One possible reason for this is that acetic acid and CO_2 produced at the cathode (due to ethanol crossover) can crossover through the membrane to the anode side, resulting in higher yields.

3.3. Performances of DEFCs with different anode catalysts

Fig. 3 shows performances of DEFCs with different anode catalysts. The same cathodes (Pt black, 4 mg cm^{-2} on carbon paper) were used in all cases. The cell was operated at 80 °C with an anode feed of 1 M ethanol(aq) and a cathode feed of dry air. It is seen that the performance of the cell with Pt/Sn, Pt/Ru, or Pt/Ru/Pb as the anode catalyst was much better than that of the cell with Pt as the anode catalyst. This indicates that Pt/Sn, Pt/Ru, and Pt/Ru/Pb catalysts have much higher catalytic activities for ethanol oxidation than the parent Pt catalyst. The higher activities can be attributed to the promoting effect of Sn, Ru, and Pb. Also, the open circuit potential (OCP) of the cell with the Pt/Sn, Pt/Ru, or Pt/Ru/Pb as the anode catalysts was much higher than that of the cell with Pt as the anode catalyst. This is due to the lower onset potential of ethanol oxidation on the Pt/Sn, Pt/Ru, and Pt/Ru/Pb catalysts [1], since the OCP for O_2 reduction should not have varied.

Another finding is that the cell with Pt/Sn as the anode catalyst had the best performance, and this is consistent with previous studies [4,5,7,9]. The peak power density of 17 mW cm^{-2} obtained with the Pt/Sn catalyst is inferior to the best literature results for ethanol/oxygen cells (40 mW cm^{-2} at 75 °C [9]), but this can be explained by our use of air as the oxidant. We have not found comparable literature data for ethanol/air cells.

With the aid of a DHE reference electrode, we have resolved cell performance dependences on two different anode catalysts into individual electrode dependences as shown in Fig. 4. It was found that the anode performance with Pt/Ru as the catalyst was much better than that with Pt as the catalyst. Therefore, it can be concluded that the better performance of the cell with Pt/Ru as the anode catalyst is mainly due to the much better anode performance.

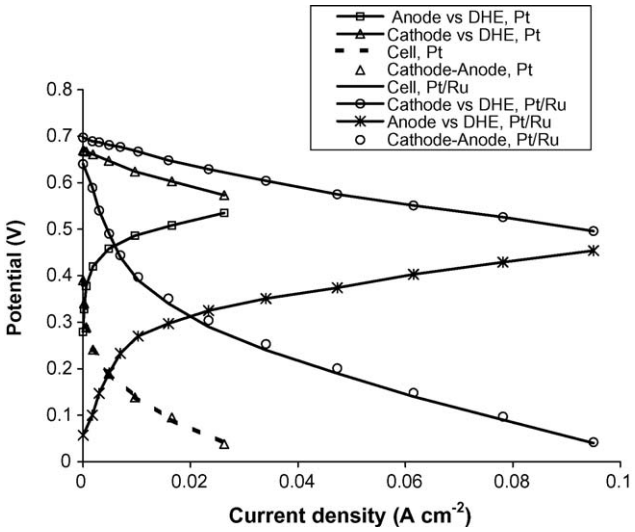

Fig. 4. Polarization curves for a DEFC with different anode catalysts of Pt and Pt/Ru, together with cathode potentials vs. DHE and anode potentials vs. DHE. The cell was operated at 80 °C with an anode feed of 1 M ethanol(aq) and a cathode feed of dry air.

We can also see that the cell polarization curves are quite close to the cathode potentials – anode potentials (versus DHE). This demonstrates the good stability of the DHE reference electrode.

3.4. Performance of DEFCs with different ethanol concentrations

Fig. 5 shows polarization curves for a DEFC with different ethanol concentrations, together with anode potentials versus DHE and cathode potentials versus DHE. It is seen that at low current densities, the cell voltage dropped rapidly with increas-

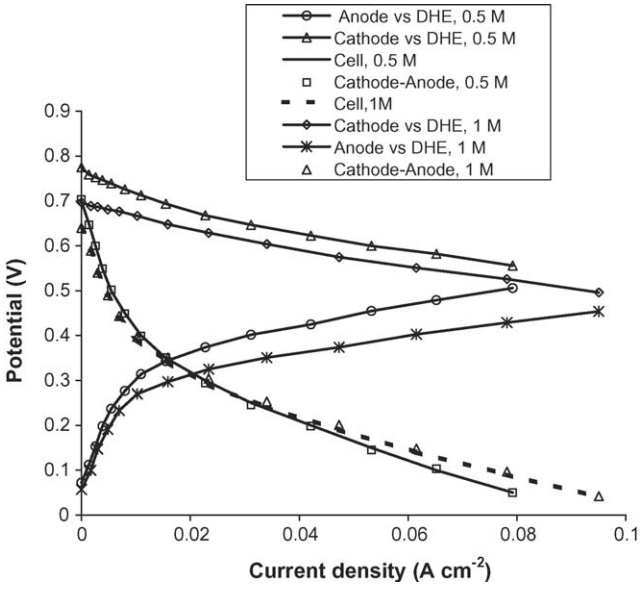

Fig. 5. Polarization curves for a DEFC at 80 °C with anode feeds of ethanol(aq) of different concentrations and a cathode feed of dry air, together with anode potentials vs. DHE and cathode potentials vs. DHE. Anode catalyst: Pt/Ru (1:1, 5.47 mg cm^{-2}).

ing current density, and the performance of the cell with 0.5 M ethanol was better than with 1 M ethanol. While at high current densities, the performance of the cell with 1 M ethanol was much better than with 0.5 M ethanol. In addition, the OCP of the cell with 0.5 M methanol was significantly higher than with 1 M ethanol. These different concentration dependences of the cell can be attributed to the different concentration dependences of the cathode and the anode.

From Fig. 5 we can see that the performance of the cathode with 0.5 M ethanol was significantly better than with 1 M ethanol. In addition, the OCP of the cathode with 0.5 M ethanol was much higher than with 1 M ethanol. These concentration dependences of the cathode are presumably due to ethanol crossover, since ethanol crossover increased significantly with increasing ethanol concentration as shown in Table 1. It is well known that methanol crossover causes depolarization of the cathode in DMFCs, resulting in significant decreases in cathode performance [31]. This effect would be expected to be more pronounced for ethanol because of the higher number of electrons involved in ethanol oxidation, and the larger number of potentially poisoning products.

However, for the anode performance, things are reversed. It can be seen from the data in Fig. 5 that the anode performance with 1 M ethanol was much better than with 0.5 M ethanol, especially at high current densities. This is due to a combination of increase of kinetics and mass transport at the higher concentration.

Another finding is that at low current densities, the anode overpotentials increased dramatically with increasing current density, while the cathode potentials dropped much more gradually with increasing current density. This indicates that the rapid drop of cell voltage at low current densities was mainly due to the rapid increase in anode overpotentials.

We can also see that there was no significant difference in OCP for the anode with the two different ethanol concentrations. Thus, the higher OCP of the cell with 0.5 M ethanol was due to the higher OCP of the cathode at the lower ethanol concentration.

Based on the different concentration dependences of the cathode and anode overpotentials, it can be concluded that a compromise between anode and cathode performance has to be made for the best cell performance.

3.5. Performance of DEFCs at different temperatures

Fig. 6 shows polarization curves for a DEFC at three different operating temperatures. It is seen that the cell performance was improved significantly at the higher temperature. However, it is also seen that the cell has the highest OCP at room temperature. Again, these temperature dependences of the cell can be attributed to the different temperature dependences of the anode and cathode.

It was found that the anode performance was improved markedly at the higher temperature (Fig. 7). Also, the OCP of the anode decreased with increasing temperature. These are understandable effects, since increasing temperature will increase the rate of ethanol oxidation and increase mass transport rates. Surprisingly, it was found that the cathode performance decreased

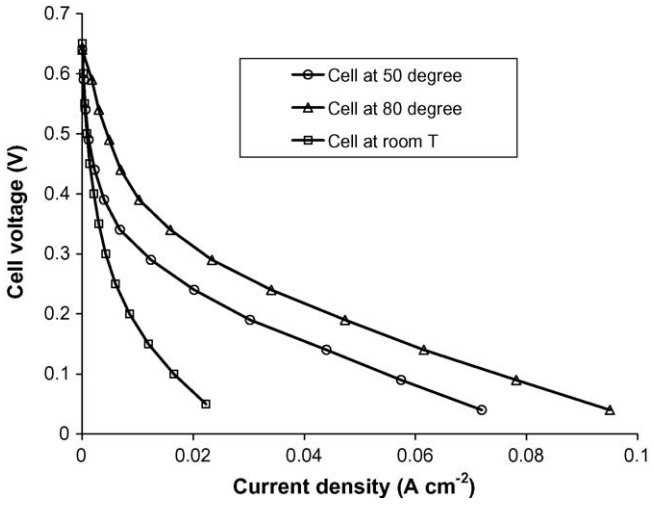

Fig. 6. Polarization curves for a DEFC at different cell operating temperatures (°C). The cell was operated with an anode feed of 1 M ethanol(aq) and a cathode feed of dry air. Anode catalyst: 5.47 mg cm^{-2} Pt/Ru (1:1).

significantly with increasing temperature as shown in Fig. 8. In addition, it can be seen that the OCP of the cathode at room temperature was much higher than at 80 °C. These results seem contradictory to the fact that increasing temperature should increase the oxygen reduction rate and mass transport rates. This contradiction suggests that other factors played more important roles.

From Table 2, we can see that ethanol crossover increased greatly with increasing temperature. Therefore, the lower cathode performance at higher temperature is likely due to the increased ethanol crossover at the higher temperature, since ethanol crossover can result in significant decreases in cathode performance. For comparison, Fig. 8 also shows a polarization curve for a cathode in a DMFC at 60 °C. It can be seen that ethanol crossover resulted in more depolarization of the cathode than methanol crossover did.

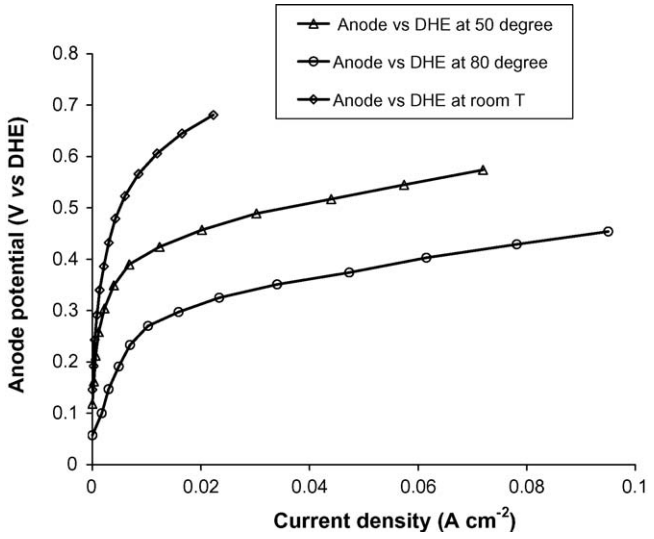

Fig. 7. Anode polarization curves of the DEFC at different temperatures. The cell operating conditions were the same as those in Fig. 6.

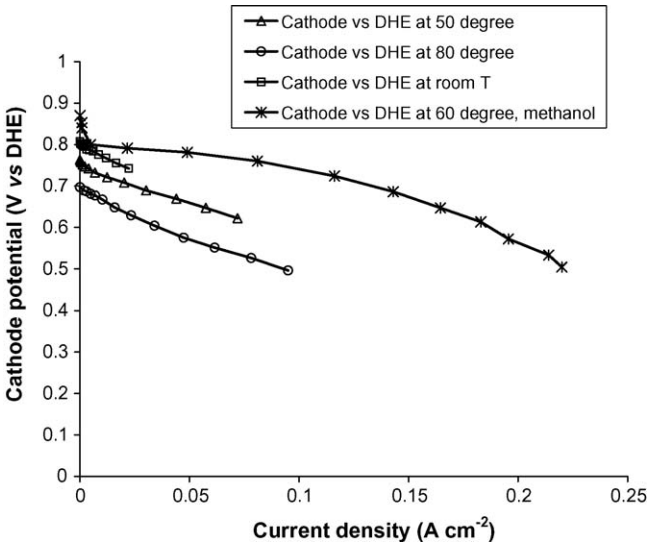

Fig. 8. Cathode polarization curves of the DEFC at different temperatures. The cell operating conditions were the same as those in Fig. 6.

The different performances of the cathode and anode at different temperatures clearly show that the better performance of the cell at the higher temperature was due to the better performance of the anode at the higher temperature.

4. Conclusions

As observed in previous studies, the performance of a DEFC has been shown to strongly depend on the anode catalyst, ethanol concentration, and operating temperature. It was found that cells with Pt/Sn, Pt/Ru, or Pt/Ru/Pb as the anode catalyst had much higher performances than a cell with Pt as the anode catalyst, with Pt/Sn giving the best performance. It has been shown that the cell performance improved markedly with increasing operating temperature. Also, it was found that at low current densities, the cell performance was better with a lower ethanol concentration, while at high current densities, the cell performance became better with a higher ethanol concentration.

Interpretation and understanding of the above effects have been enhanced with the aid of a DHE reference electrode, which has allowed cell performance losses to be separated into components due to the cathode and anode. Many features of the operation for DEFCs inferred from previous studies of cell potentials have been confirmed by the single electrode results, and new insights have arisen. In particular, it was found that the cathode and anode depended differently on ethanol concentration and operating temperature.

The performance analysis illustrated that the anode performance was improved with increasing temperature and ethanol concentration, while the cathode performance decreased with increasing temperature and ethanol concentration. Therefore, a balance between the anode and the cathode has to be made for the best cell performance.

Product analysis demonstrated that CO_2 was not the main product of ethanol oxidation under the conditions used here. It was found that the yield of CO_2 did not change significantly with cell voltage, while the yield of acetic acid changed significantly with cell voltage.

Acknowledgements

This work was supported by the Natural Sciences and Engineering Research Council of Canada and Memorial University. We thank Ballard Power Systems and H. Power Corp. for donation of materials for construction of MEAs.

References

[1] C. Lamy, A. Lima, V. LeRhun, F. Delime, C. Coutanceau, J.M. Leger, J. Power Sources 105 (2002) 283.
[2] A.S. Arico, P. Creti, P.L. Antonucci, V. Antonucci, Electrochem. Solid State Lett. 1 (1998) 66.
[3] W.J. Zhou, Z.H. Zhou, S.Q. Song, W.Z. Li, G.Q. Sun, P. Tsiakaras, Q. Xin, Appl. Catal. B Environ. 46 (2003) 273.
[4] F. Vigier, C. Coutanceau, A. Perrard, E.M. Belgsir, C. Lamy, J. Appl. Electrochem. 34 (2004) 439.
[5] W.J. Zhou, B. Zhou, W.Z. Li, Z.H. Zhou, S.Q. Song, G.Q. Sun, Q. Xin, S. Douvartzides, A. Goula, P. Tsiakaras, J. Power Sources 126 (2004) 16.
[6] C. Lamy, S. Rousseau, E.M. Belgsir, C. Coutanceau, J.-M. Leger, Electrochim. Acta 49 (2004) 3901.
[7] W.J. Zhou, W.Z. Li, S.Q. Song, Z.H. Zhou, L.H. Jiang, G.Q. Sun, Q. Xin, K. Poulianitis, S. Kontou, P. Tsiakaras, J. Power Sources 131 (2004) 217.
[8] S. Song, W. Zhou, J. Tian, R. Cai, G. Sun, Q. Xin, S. Kontou, P. Tsiakaras, J. Power Sources 145 (2005) 266.
[9] W.J. Zhou, S.Q. Song, W.Z. Li, Z.H. Zhou, G.Q. Sun, Q. Xin, S. Douvartzides, P. Tsiakaras, J. Power Sources 140 (2005) 50.
[10] S.Q. Song, W.J. Zhou, Z.H. Zhou, L.H. Jiang, G.Q. Sun, Q. Xin, V. Leontidis, S. Kontou, P. Tsiakaras, Int. J. Hydrogen Energy 30 (2005) 995.
[11] J. Wang, S. Wasmus, R.F. Savinell, J. Electrochem. Soc. 142 (1995) 4218.
[12] E. Casado-Rivera, D.J. Volpe, L. Alden, C. Lind, C. Downie, T. Vazquez-Alvarez, A.C.D. Angelo, F.J. DiSalvo, H.D. Abruna, J. Am. Chem. Soc. 126 (2004) 4043.
[13] A.O. Neto, M.J. Giz, J. Perez, E.A. Ticianelli, E.R. Gonzalez, J. Electrochem. Soc. 149 (2002) A272.
[14] J.P.I. deSouza, S.L. Queiroz, K. Bergamaski, E.R. Gonzalez, F.C. Nart, J. Phys. Chem. B 106 (2002) 9825.
[15] V.P. Santos, V. Del Colle, R.B. de Lima, G. Tremiliosi-Filho, Langmuir 20 (2004) 11064.
[16] H. Wang, Z. Jusys, R.J. Behm, J. Phys. Chem. B 108 (2004) 19413.
[17] S. Tanaka, M. Umeda, H. Ojima, Y. Usui, O. Kimura, I. Uchida, J. Power Sources 152 (2005) 34.
[18] S. Jayaraman, A.C. Hillier, Meas. Sci. Technol. 16 (2005) 5.
[19] E.V. Spinace, M. Linardi, A.O. Neto, Electrochem. Commun. 7 (2005) 365.
[20] C.W. Xu, P.K. Shen, J. Power Sources 142 (2005) 27.
[21] Y.X. Bai, J.J. Wu, J.Y. Xi, J.S. Wang, W.T. Zhu, L.Q. Chen, X.P. Qiu, Electrochem. Commun. 7 (2005) 1087.
[22] C.W. Xu, P.K. Shen, X.H. Ji, R. Zeng, Y.L. Liu, Electrochem. Commun. 7 (2005) 1305.
[23] N. Fujiwara, K.A. Friedrich, U. Stimming, J. Electroanal. Chem. 472 (1999) 120.
[24] M.J. Gonzalez, C.T. Hable, M.S. Wrighton, J. Phys. Chem. B 102 (1998) 9881.
[25] F. Vigier, C. Coutanceau, F. Hahn, E.M. Belgsir, C. Lamy, J. Electroanal. Chem. 563 (2004) 81.
[26] V.P. Santos, G. TremiliosiFilho, J. Electroanal. Chem. 554 (2003) 395.
[27] A. Heinzel, V.M. Barragan, J. Power Sources 84 (1999) 70.

[28] M.A. Hickner, H. Ghassemi, Y.S. Kim, B.R. Einsla, J.E. McGrath, Chem. Rev. 104 (2004) 4587.
[29] S. Song, G. Wang, W. Zhou, X. Zhao, G. Sun, Q. Xin, S. Kontou, P. Tsiakaras, J. Power Sources 140 (2005) 103.
[30] V. Paganin, E. Sitta, T. Iwasita, W. Vielstich, J. Appl. Electrochem. 35 (2005) 1239.
[31] G. Li, P.G. Pickup, Electrochim. Acta 49 (2004) 4119.
[32] X. Ren, T.E. Springer, S. Gottesfeld, J. Electrochem. Soc. 147 (2000) 92.
[33] C.M. Davis, M.C. Mauck, J. Chem. Educ. 80 (2003) 552.
[34] K.M. Keener, J.D. LaCrosse, J.K. Babson, Poultry Sci. 80 (2001) 983.
[35] J. Zhu, R.R. Sattler, A. Garsuch, O. Yepez, P.G. Pickup, Electrochim. Acta, in press.